

Monitoring and Detecting the Impact of Oil Sabotage on Land Using Multispectral Imagery

Okechukwu Okpobiri^{1*}, Ayowei Alvin Harry²

¹Department of Geology, Rivers State University, Nigeria. 500001

²Department of Environment University of Salford, London UK. M5 4WT

Email address: okechukwuokpobiri(at)yemail.com, ayoweialvin(at)gmail.com

Abstract— Oil pollution has been shown to cause ecological imbalances in the Niger Delta region. The most efficient method of detecting and quantifying oil spill extent, assessing the impact of these spills, and predicting remediation measures is to use multispectral imagery with a geospatial tool. The data was obtained from the Nigeria Oil Spill Detection and Response Agency (NOSDRA) between January and April 2019, and the US Geological Survey provided Landsat 5 in 1990 and Landsat 8 in 2020. This study assesses the spatial and temporal impact of sabotage spillage in 34 locations. The results show that the total oil spill on land is 70%, while the recovered oil spill is 30%, implying that 40% of the oil spill is spread across the study area, causing environmental pollution. The impact of spills on vegetation is calculated using vegetation indices based on the spectral bands most sensitive to plants and soil, namely the Near Infrared (NIR), Red (R), and Green (G) bands. This study used five indices: the Normalized Difference Vegetation Index (NDVI), the Soil Adjusted Vegetation Index (SAVI), the Atmospheric Resistant Vegetation Index 2 (ARVI2), the Green-Short Wave Infrared (G-SWIR), and the Green-Near Infrared (GNIR) (G-NIR). The NDVI decreases slightly from 0.19–0.2 to 0.14–0.18, while the SAVI decreases significantly from 0.31–0.65 to 0.21–0.27. The ARVI2 decreases from 0.06–0.33 to -0.01–0.03 between 1990 and 2020, while the G-SWIR decreases from -0.15–0.11 to -0.1–0.16. The G-NIR however increases from 0–0.01 to 0.05–0.08. The large variance in the spatiotemporal analysis of these vegetation indices indicates environmental degradation.

Keywords— Broadband Multispectral Vegetation indices (BMVI), Sabotage, Oil spill, Ecological; imbalance; NOSDRA.

I. INTRODUCTION

The Niger Delta region has been plagued with oil spill since 1958 when Nigeria joined the World's rank of oil producers. Over 10% of the total amount of oil spilled have not been recovered (Abii 2009). Conventional field methods of detecting and mapping oil spill trajectory though effective, is Traditional field methods of detecting and mapping oil spill trajectories, while effective, are time-consuming, costly, and have limited spatial coverage, resulting in an underestimation of spill areas. Despite the fact that most areas have remediation activities in place, these environmental stressors disrupt ecological balance. Because spill oil rarely spreads far in the terrestrial environment, the first noticeable effect of an oil spill on land is vegetation (Nelson 1979). (UNEP 2011) stated that, while different vegetation types respond differently to hydrocarbons, the formation of free radicals in plant cells occurs when oxygen and other nutrients are displaced by oil that has percolated the soil. Pavanelli and Loch (2018) observed a decline in vegetation health in two different locations in Brazil 40 days after the spill.

According to the study, the impact of an oil spill on vegetation is determined by the level of exposure and the chemistry of the oil. Plants absorb and reflect specific spectral bands in the electromagnetic spectrum, so monitoring vegetation cover is critical. These radiations are influenced by pigment (chlorophyll) concentration, cellular structure, leaf anatomy, and moisture content (Onyia et al., 2019; clevers 2002). The use of remote sensing in conjunction with GIS is a more efficient method of surveying and mapping these spills. They are also used in environmental impact assessment, where the Broadband Multispectral Vegetative Index, a tool that quantifies vegetation biomass using reflected spectral bands, is used. The most commonly used indices are the Normalised Difference Vegetation Index (NDVI) and the Soil Adjusted Vegetation Index (SAVI).

II. THE STUDY AREA

The study area is located within longitudes 6°24'0" E and 6°52'0" E and latitude 5° 0'0"N and 5° 20'0"N in (Figure 1). The topography is usually low-lying with altitude ranging from beneath sea level in the southwestern flank of the location to about 39 m (Eteh and Okechukwu. 2021) similarly inland. The average rainfall and temperature of the area are 2,899 mm and 26.7 °C respectively. The area is drained with the aid of tributaries and creeks such as Taylor creek linked to Orashi River respectively. Some sections of the study area are on land and could be accessed by road, with numerous hydrocarbon flow stations owned by the SPDC and Agip Oil Company.

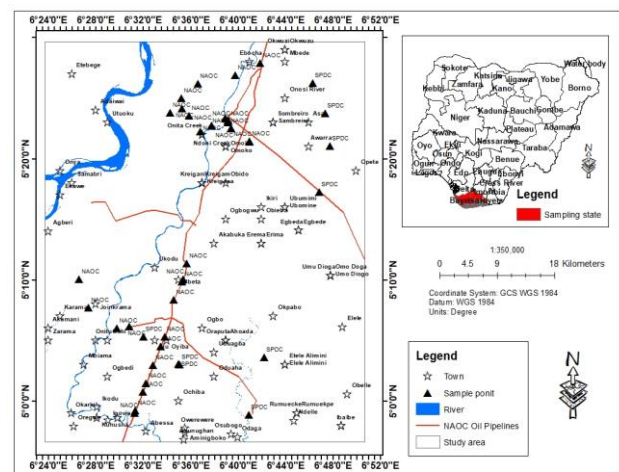


Fig. 1. Location of study area

III. MATERIALS AND METHODS

Data Set

Multispectral imageries from Landsat 5 in 1990 and Landsat 8 in 2020 were obtained from <https://earthexplorer.usgs.gov/> as shown in table 1. Additional data are oil spill records for 34 spill points and their Global Positioning System (GPS) location from January to April 2019 got from Nigeria Oil Spill Detection and Response Agency (NOSDRA) archives at <https://oilspillmonitor.ng/#/>. See Tables 4, 5, 6 and 7.

TABLE 1: List of Satellite Data collected

Satellite Data	Date	Spatial Resolution (m)	Source
Landsat 5	09/12/1990 Path: 189, Row: 57	30	https://earthexplorer.usgs.gov/
Landsat 8	6/12/2020 Path: 189, Row: 56	30	https://earthexplorer.usgs.gov/

Limitation

In order to minimize the effect of cloud cover, in Landsat 8, this study is limited to the months January to April 2019 as there is less cloud cover at this time of the year.

Data processing

The spill data in degrees, minutes, and seconds acquired from Nigeria Oil Spill Detection Response Agency (NOSDRA), was imported into Microsoft Excel and converted to degree decimal before it was loaded into the Geographical Information System environment in Database Format to produce a sample location map using Arc GIS software. The Arc GIS spatial analyst extension was used to generate the pollution map of oil spilled, oil recovered and oil injected into the ecosystem. Integration of data visualization from January to April 2019 using quantitative analysis in ArcGIS software symbols and then, Map algebra in raster calculator, various vegetation indices such as NDVI, SAVI, ARVI2, G-NIR, and G-SWIR were derived. Finally, statistical analysis of the data for estimated oil spilled and recovered on the base of the count, minimum, maximum, sum, mean is used to plot of bar and pie chart.

Vegetation Indices

The use of Landsat imagery for the detection of oil spill and its impact on vegetation via vegetation indices derived from broadband multispectral data is vital for environmental study. The study utilizes five vegetation stress derived from Landsat 5 in Table 3 and Landsat 8 in 2 sensors.

TABLE 2: Spectral bands in Landsat 8 for vegetation indices

Band no	Description	Wavelength (µm)	Resolution (m)
2	visible blue	0.450 to 0.515	30
3	visible green	0.525 to 0.6	30
4	visible red	0.630 to 0.68	30
5	Near-Infrared	0.845 to 0.885	30
6	Short-wave infrared I	1.56 to 1.66	30

TABLE 3: Spectral bands in Landsat 5 for vegetation indices

Band no	Description	Wavelength (µm)	Resolution (m)
1	visible blue	0.450 to 0.515	30
2	visible green	0.525 to 0.6	30
3	visible red	0.630 to 0.69	30
4	Near-Infrared	0.77 to 0.90	30
5	Short-wave infrared I	1.55 to 1.75	30

Atmospheric correction

The formulas for atmospheric correction of Landsat-8 imager from Digital Number (DN) to Top of Atmosphere (TOA) reflectance using reflectance rescaling coefficients from Landsat-8 metadata file are presented in equations 1 and 2.

$$P\lambda = M_p Q_{cal} + A_p \tag{1}$$

where: $\rho\lambda'$ TOA is the planetary reflectance without correction for the solar angle., M_p Band-specific multiplicative rescaling factor from the metadata, A_p Band-specific additive rescaling factor from the metadata,

Q_{cal} = Quantized and calibrated standard product pixel values (DN).

TOA reflectance corrected for the sun angle is:

$$p\lambda = \frac{\rho\lambda}{\cos(\theta_{sz})} = \frac{\rho\lambda}{\cos(\theta_{se})} \tag{2}$$

Normalized Difference Vegetation index

NDVI has been shown to demonstrate unique spectral characteristics for the detection of vegetation stress. The red band in the visible spectrum is sensitive to chlorophyll content and a high reflection of NIR characterizes healthy vegetation conditions. The index has been successfully used for characterizing vegetation cover and is still considered a great potential for application in environmental monitoring because of its low cost compared to hyperspectral data (Rouse et al. 1973; Running et al. 1994).

$$NDVI = (R_{NIR} - R_{RED}) / (R_{NIR} + R_{RED}) \tag{3}$$

Soil Adjusted Vegetation Index

The SAVI index developed by Huete (1988) and Huete et al. (1992) incorporated an adjustment factor of canopy background and atmospheric conditions to address noise found in NDVI. This index is useful for correcting the soil brightness factor and atmospheric effects (Rondeaux, et al. 1996).

$$SAVI = ((R_{NIR} - R_{RED}) / (R_{NIR} + R_{RED} + 0.5)) \times (1 + 0.5) \tag{4}$$

Atmospheric Resistant Vegetation Index 2

The ARVI2 index was designed to be resistant to atmospheric effects and more sensitive to a wide range of chlorophyll concentrations. Both NDVI and ARVI2 are sensitive to vegetation fraction and to the rate of absorption of photosynthetic solar radiation (Gitelson, et al., 1996; Kaufman and Tanre 1992).

$$ARVI2 = -0.18 + 1.17 \times (R_{NIR} - R_{RED} / R_{NIR} + R_{RED}) \tag{5}$$

Green-Near Infrared

The G-NIR index is a simple combination of green and near-infrared reflectance values. The green band has the capacity to assess plant vigour while the NIR characterize vegetation internal structure (Sripada et al. 2005). It has also shown a potential to discriminate between vegetation affected by oil spill and unaffected sites both spatially and temporally (Adamu, et al. 2015).

$$G-NIR = (R_{GREEN} - R_{NIR}) / (R_{GREEN} + R_{NIR}) \tag{6}$$

Green-Short-wave Infrared

The G-SWIR index have a capacity to predict and sense nitrogen in plants (Herrmann *et al.* 2010). SWIR is also capable of discriminating moisture content of soil and vegetation

(Karnieli *et al.* 2001) therefore G-SWIR could be useful in detecting changes in vegetation affected by an oil spill.

$$G-SWIR = (R_{GREEN} - R_{SWIR}) / (R_{GREEN} + R_{SWIR})$$

7

IV. RESULT AND DISCUSSION

TABLE 4. Oil spill data for January 2019 from Nigeria Oil Spill Detection and Response Agency (NOSDRA)

ID	Status	Company	Incident no	Incident date	Estimated oil Spill (bbl)	Recovery (bbl)	Facility	Cause	Latitude	Longitude
145880	confirmed	NAOC	2019/LAR/020/029	2019-01-28	0.9153	0	Fl	sab	5.393194	6.598167
145879	confirmed	NAOC	2019/LAR/021/031	2019-01-28	2.7	2	Fl	sab	5.375639	6.656722
145821	confirmed	NAOC	2019/LAR/018/025	2019-01-24	3.8	2	Fl	sab	5.389583	6.648556
145819	confirmed	NAOC	2019/LAR/017/023	2019-01-22	0.17	0	Fl	sab	5.417389	6.587361
145817	confirmed	NAOC	2019/LAR/016/021	2019-01-21	7.2	4	Fl	sab	5.375611	6.656722
145822	confirmed	NAOC	2019/LAR/014/019	2019-01-16	8	5	Fl	sab	5.465778	6.697556
145772	confirmed	NAOC	2019/LAR/012/017	2019-01-16	279.41	230	Pl	sab	5.102639	6.513444
170340	confirmed	NAOC	2019/LAR/011/013	2019-01-10	7.04	0	Pl	sab	5.167583	6.589444
145741	confirmed	NAOC	2019/LAR/010/012	2019-01-10	0.16	0	Fl	sab	5.448667	6.663111
145424	confirmed	NAOC	2019/LAR/008/009	2019-01-06	7.28	0	Pl	sab	5.139722	6.576111
145293	confirmed	NAOC	2019/LAR/007/008	2019-01-06	373	252	Wh	sab	5.357278	6.682972
145275	confirmed	NAOC	2019/LAR/005/005	2019-01-04	2.4	0	Fl	sab	5.370889	6.61375
145285	confirmed	NAOC	2019/LAR/002/002	2019-01-03	0.4	0	Fl	sab	5.379361	6.629222
145426	confirmed	NAOC	2019/LAR/001/001	2019-01-02	10	0	Fl	sab	5.100639	6.496333
145287	confirmed	NAOC	2019/LAR/004/004	2019-01-02	0.63	0	Pl	sab	4.983694	6.521083
145284	confirmed	NAOC	2019/LAR/003/003	2019-01-02	0.15	0	Pl	sab	4.986972	6.522389
145937	confirmed	SPDC	2252623	2019-01-26	45	19	Pl	sab	5.438077	6.77165
145990	confirmed	SPDC	2222867	2019-01-17	0.48	0	Pl	sab	4.98149	6.68163
145431	confirmed	SPDC	2243182	2019-01-09	535	220	Pl	sab	5.05013	6.58413

TABLE 5. Oil spill data for February 2019 from Nigeria Oil Spill Detection and Response Agency (NOSDRA)

ID	Status	Company	Incident no	Incident date	Estimated oil Spill(bbl)	Recovery (bbl)	Facility	Cause	Latitude	Longitude
146018	confirmed	NAOC	2019/LAR/026/045	2019-02-25	5	0	Fl	sab	5.386667	6.652667
146890	confirmed	SPDC	2272155	2019-02-25	288	112	Pl	sab	5.05129	6.583

TABLE 6. Oil spill data for March 2019 from Nigeria Oil Spill Detection and Response Agency (NOSDRA)

ID	Status	Company	Incident no	Incident date	Estimated oil Spill (bbl)	Recovery (bbl)	Facility	Cause	Latitude	Longitude
147927	confirmed	NAOC	2019/LAR/034/061	2019-03-29	7	2	Fl	Sab	5.403139	6.588167
170331	confirmed	NAOC	2019/LAR/031/056	2019-03-22	0.465		Fl	Sab	5.436944	6.609972
170329	confirmed	NAOC	2019/LAR/032/057	2019-03-22	0.6		Fl	Cor	5.397139	6.571167
146075	confirmed	NAOC	2019/LAR/030/053	2019-03-05	10	5	Fl	Sab	5.3755	6.656889

TABLE 7. Oil spill data for April 2019 from Nigeria Oil Spill Detection and Response Agency (NOSDRA)

ID	Status	Company	Incident no	Incident date	Estimated oil Spill(bbl)	Recovery(bbl)	Facility	Cause	Latitude	Longitude
169014	confirmed	NAOC	2019/LAR/053/093	43582	1.1	0	Pl	sab	5.189472	6.594694
169013	confirmed	NAOC	2019/LAR/052/090	43582	1.05	0	Pl	sab	5.164111	6.587722
168977	confirmed	NAOC	2019/LAR/051/088	43581	10.064	9.5	Pl	sab	5.012528	6.532472
170061	confirmed	NAOC	2019/LAR/048/081	43569	14.22	10	Fl	sab	5.3755	6.656917
170037	confirmed	NAOC	2019/LAR/045/078	43566	43.608	0	Fl	sab	5.38375	6.652694
170036	confirmed	NAOC	2019/LAR/043/075	43566	27.49	0	Fl	sab	5.385611	6.652667
170035	confirmed	NAOC	2019/LAR/044/077	43566	27.49	0	Fl	sab	5.385639	6.652667
190475	confirmed	NAOC	2019/LAR/047	43564	3	0	Fl	sab	5.129028	6.456028
159894	confirmed	NAOC	2019/LAR/041/071	43560	0.61	0.25	Pl	sab	5.049306	6.54725
156539	confirmed	NAOC	2019/LAR/040/070	43560	0.15	0	Pl	sab	5.089056	6.563306
153526	confirmed	NAOC	2019/LAR/038/067	43560	120.8	0	Pl	sab	5.0245	6.537306
153522	confirmed	NAOC	2019/LAR/039/069	43560	3.2	0	Pl	sab	5.075444	6.557861
168986	confirmed	NAOC	2019/LAR/042	43559	2	0	Fl	sab	5.167694	6.442528
153594	confirmed	NAOC	2019/LAR/035/064	43559	8	6.5	Fl	sab	5.357667	6.682722
170092	confirmed	SPDC	2331302	43579	150	0	Pl	sab	5.08878	6.53346
166268	confirmed	SPDC	2325757	43571	5	0	Pl	sab	5.3508	6.79583
166313	confirmed	SPDC	2019_2325957	43570	1	0	Pl	sab	5.06068	6.70377
166254	confirmed	SPDC	2317463	43556	10	5	Pl	sab	5.396472	6.789333

The Environmental Consequences of Oil Spill Sabotage on Land Area

The environmental implications of oil spills on land areas have always been a major challenge within the Niger Delta region. Some of which include poor health arising from the consumption of contaminated groundwater and poor crop yield. These justify the need for a response to oil spills and the need for International Oil Companies and the Federal Government to bridge the gap in providing appropriate security in land areas such as flow lines, pipelines, and truck lines.

TABLE 8: Estimated oil spill and recovered in study area.

Estimated spill	NAOC		SPDC	
	Jan-19	Feb-19	Jan-19	Feb-19
No of incident	16	1	16	1
Min	0.15	0.46	0	2
Max	373	10	252	5
Sum	703.25	18.06	495	7
Mean	43.95	4.52	30.94	3.5
Mar-19				
No of incident	4	4	4	4
Min	0.15	1	0	0
Max	120.8	150	10	5
Sum	267.78	166	26.25	5
Mean	18.77	41.5	1.87	1.25
Apr-19				
No of incident	14	4	14	4
Min	0.15	1	0	0
Max	120.8	150	10	5
Sum	267.78	166	26.25	5
Mean	18.77	41.5	1.87	1.25

Oil spill management and response

Poor management of oil spill response and recovery is one of the most important challenges facing Nigeria's oil industry, according to the World Health Organization (WHO) 2011 in the country. Oil pollution has been shown to cause ecological imbalance, resulting in poor vegetation performance due to a lack of proper management. Oil spill response is important when it comes to managing oil spills. The results from Tables 4, 5, 6, and 7 were obtained from NOSDRA, which is being analyzed to understand how oil spills are managed in our environment. Therefore, Table 8 shows that in January 2019, the total number of incidents that occurred was 16, with an estimated oil spill by NAOC of 703.25bbl while the recovery was 495bbl. Figure 2 and Figure 3a indicate 59% of the estimated oil spill on land by NAOC in the study area and 41% recovery in January 2019. Table 8 also indicates for SPDC that in January 2019 the total number of incidents that occurred was

3, with an estimated oil spill of 508.48 bbl while the recovery was 239.01 bbl. Figure 2 and Figure 3b indicate 71% of the estimated oil spill on land by SPDC in the study area and 29% recovery in January 2019. Also from the spatial analysis of oil spills, the pollution map in Figure 7 shows how the spill is spread across the study and the environmental implications of the quantity of oil spilled that is not recovered lead to environmental pollution.

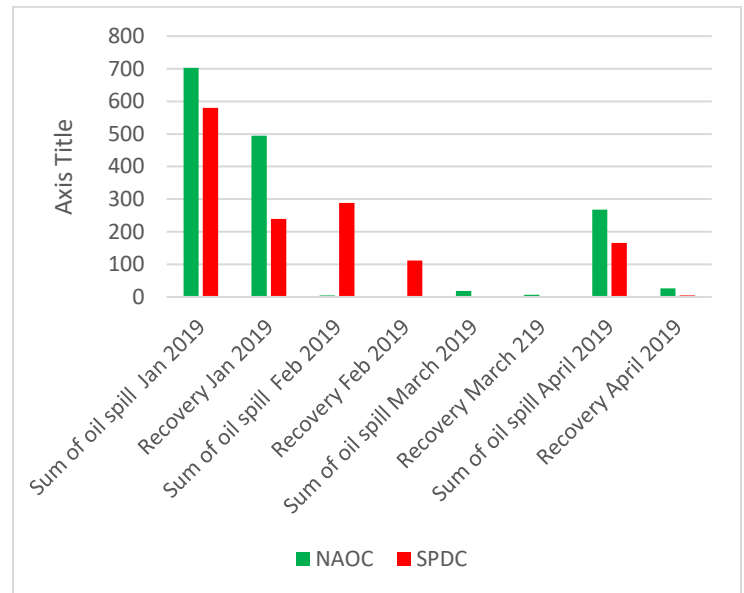


Fig. 2. Estimated oil spilled and recovered from January – April 2019

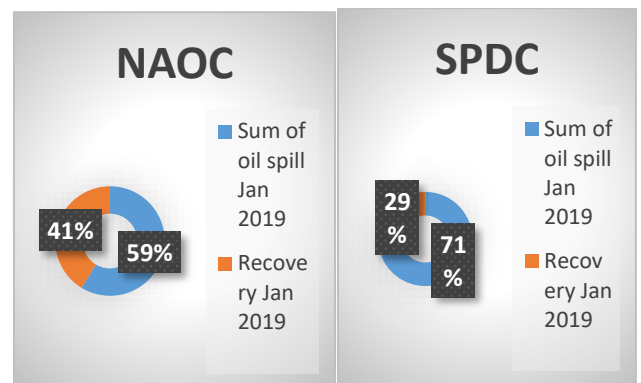


Fig. 3a and b Percentage of oil spilled and recovered by both IOCs in January 2019.

Table 8 reveals that in February 2019, there was a total of 1 event, with an estimated oil spill of 5 bbl by NAOC and a zero bbl recovery. Figures 2 and 4a show that NAOC projected a 100 percent oil leak on land in the study region in February 2019, with a 0 percent recovery. Table 8 also shows that in February 2019, SPDC had a total of 1 event, with an estimated oil spill of 288 bbl and a recovery of 112 bbl. Figure 2 and Figure 4b indicate 72% of the estimated oil spill on land by SPDC in the study area and a 28% recovery in February 2019. Also, the spatio-temporal map of oil spill distribution in Figure 9 shows how the spill is spread across the study area, indicated in blue.

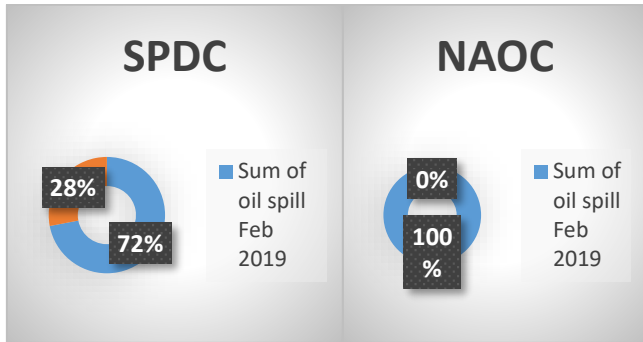


Fig. 4a and b Percentage of oil spilled and recovered by both IOCs in February, 2019

According to Table 8, there were 4 events in March 2019, with an estimated oil leak of 18.06 bbl by NAOC, with a minimum value of 0.46 bbl and a maximum value of 10 bbl, including a mean value of 4.52 bbl, and a recovery of 7 bbl. Figures 2 and 5 show that NAOC assessed a 70 percent oil spill on land in the study region, with a 27 percent recovery rate in March 2019. While there was no spill occurrence for SPDC in March 2019. In addition, the qualitative map of oil spill distribution in Figure 9 indicates how the spill is distributed across the study, with red showing the location of the spill.

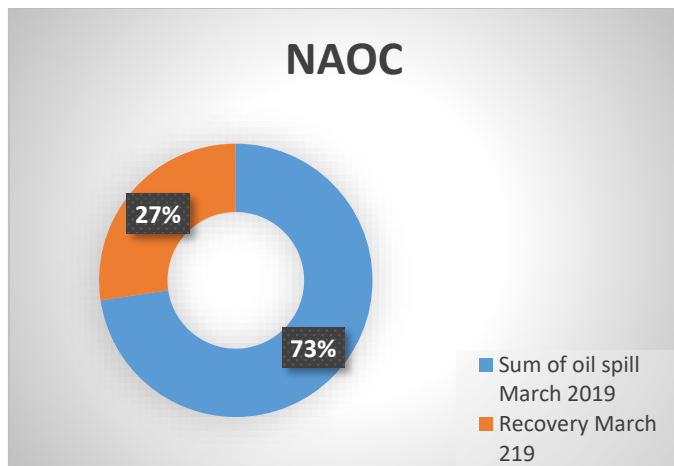


Fig. 5. Percentage of oil spilled and recovered by NAOC in March, 2019

According to Table 8, the total number of incidents that occurred in April 2019 was 14. NAOC's estimated oil spill was 267.78 bbl, with a recovery of 26.25 bbl. Figures 2 and 6a show that NAOC estimated 91 percent of the oil spill on land in the study area and a 9 percent recovery in April 2019. While Table 8 shows that SPDC had four incidents in April 2019, with an

estimated oil spill of 166 bbl and a recovery of 5 bbl, Figures 2 and 6b show that SPDC had 97 percent of the estimated oil spill on land in the study area and a 3 percent recovery in April 2019. Furthermore, according to the qualitative map of oil spill distribution in Figure 9, the spill is distributed throughout the study, indicating green, and the environmental implications of the quantity of oil spilled that is not recovered lead to environmental pollution. The total estimated oil spill for NAOC and SPDC from January to April 2019 is 70%, while recovery is 30%, meaning 40% is spread across the environment (Fig 7).

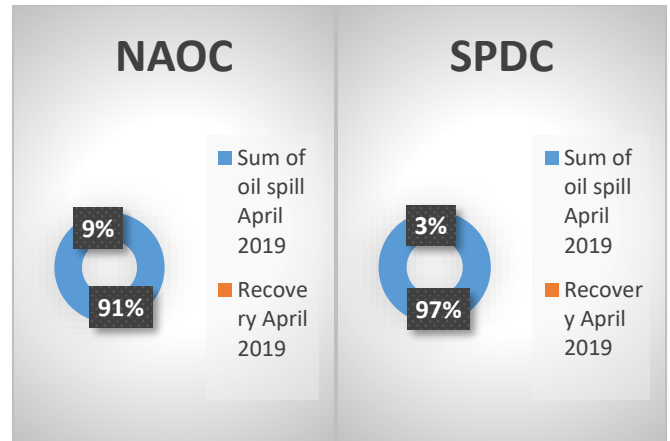


Fig. 6a and 6b Percentage of Oil spilled and recovered by SPDC in April, 2019

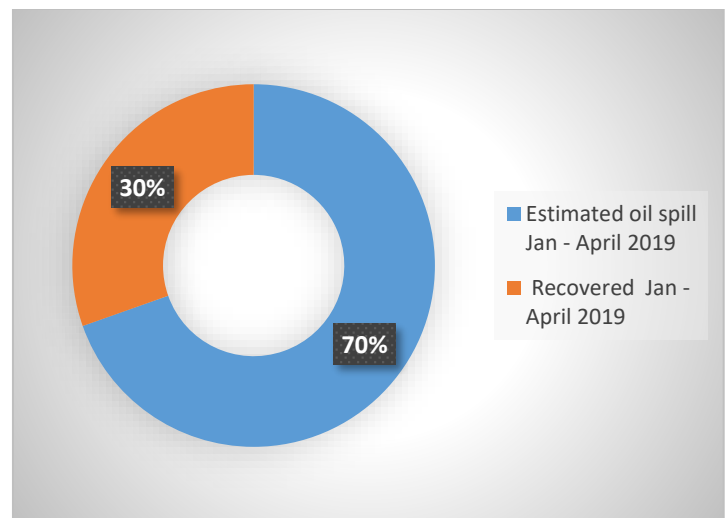


Fig. 7. Total Percentage of Oil spilled and recovered by NAOC and SPDC from January to April, 2019.

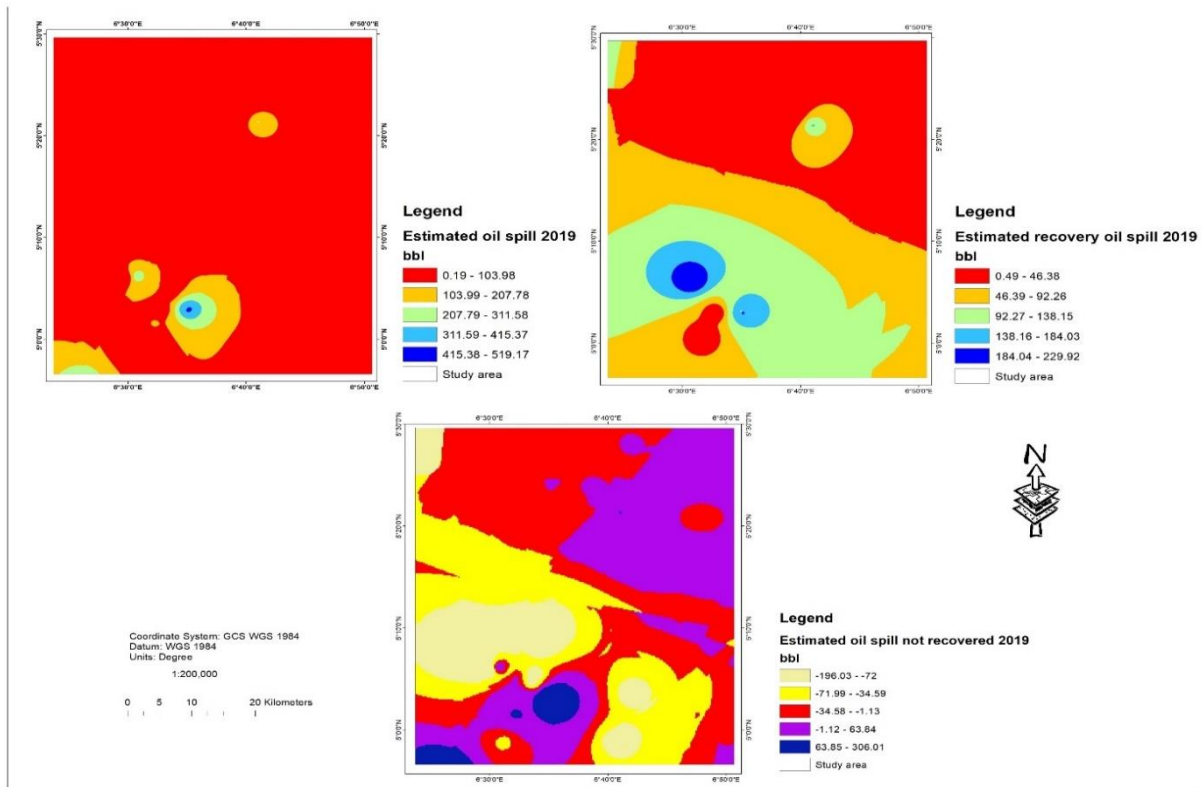


Fig. 8. Spatial oil spill Pollution map showing, estimated oil spill. Recovered and lost from January – April 2019.

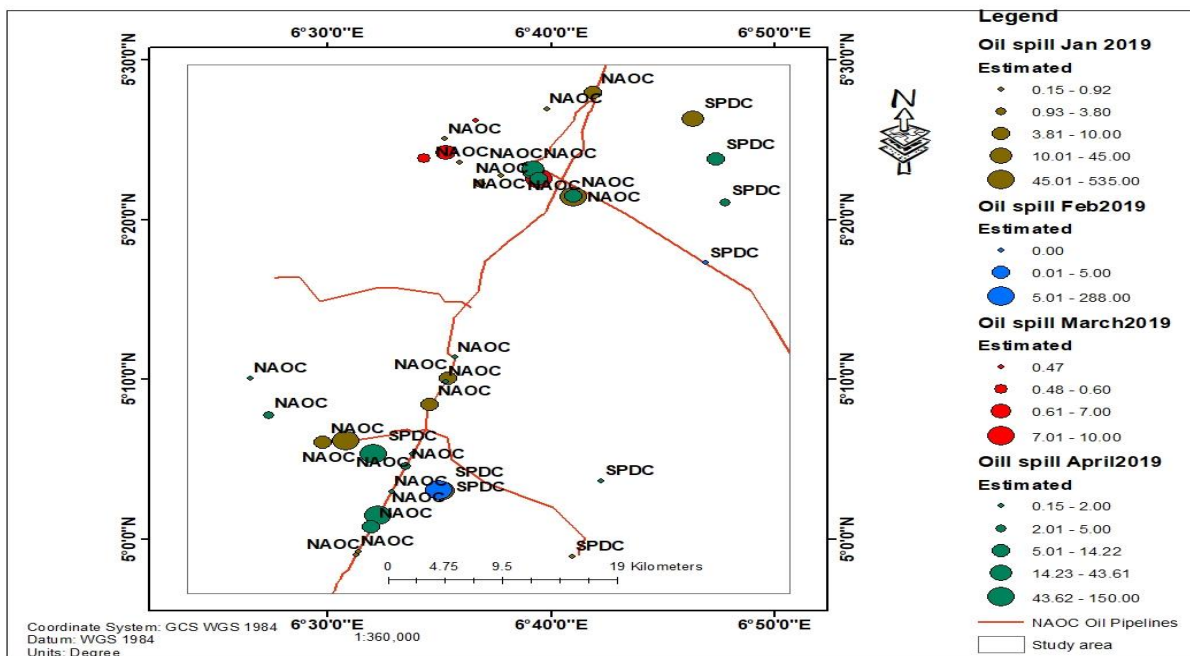


Fig. 9. Spatiotemporal analysis map

Using the vegetation index to assess the impact of an oil spill on land.

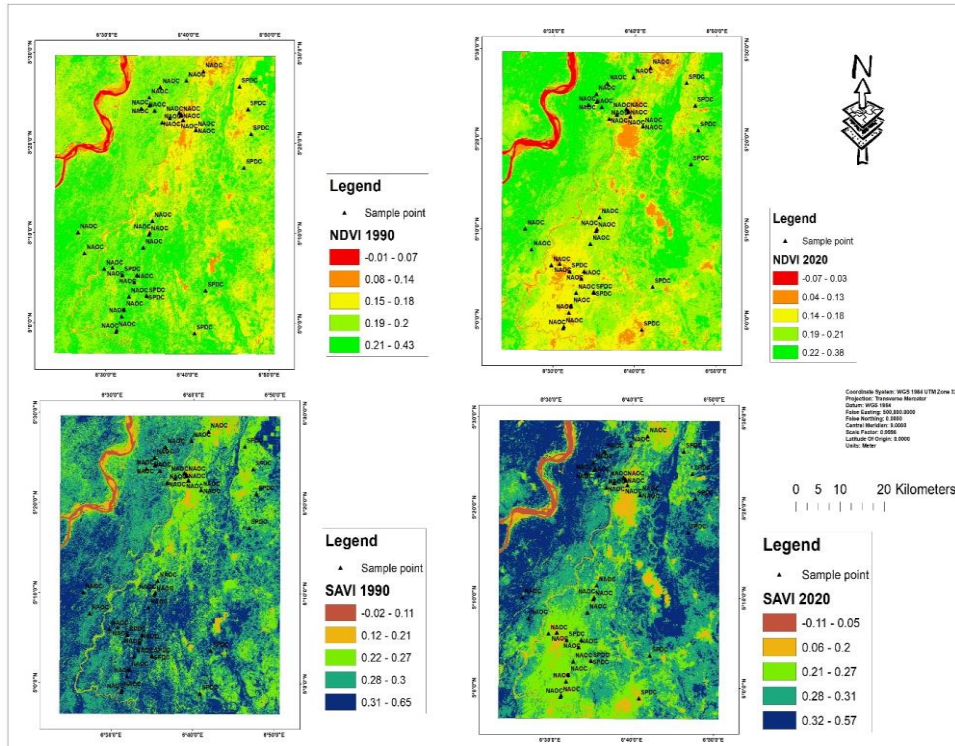


Fig. 10. Vegetation analysis of NDVI and SAVI

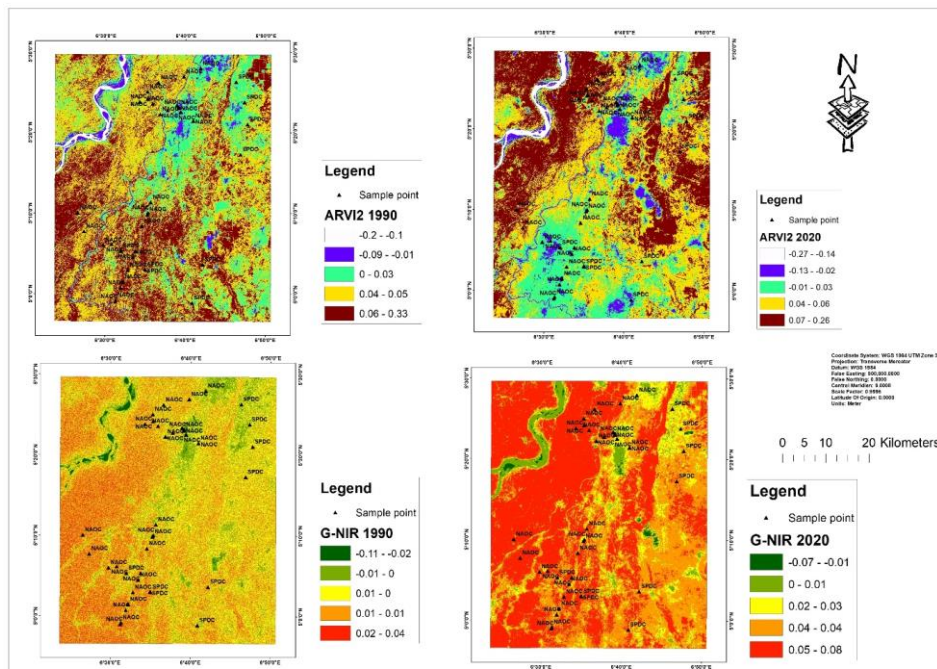


Fig. 11. Vegetation analysis of ARVI2 and G-NIR for 1990 and 2020

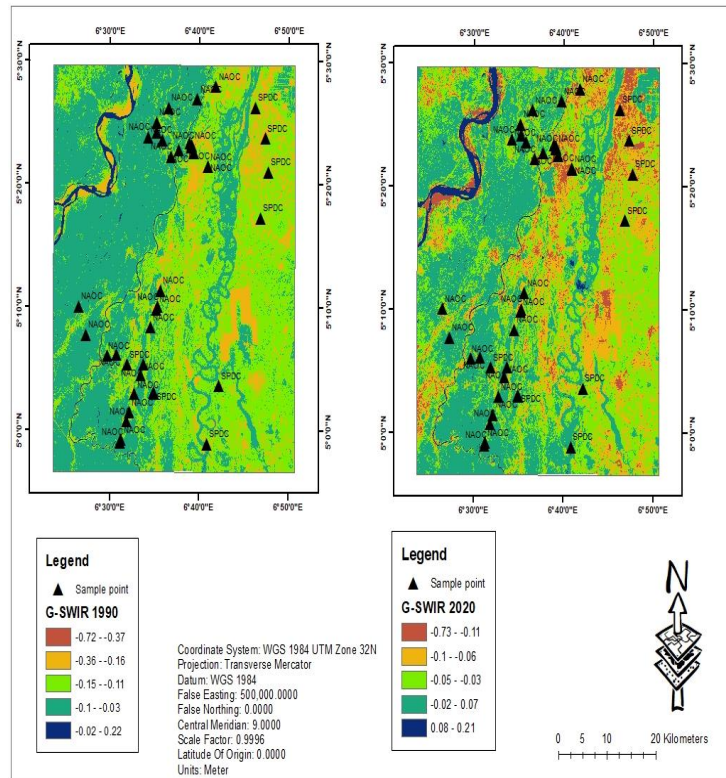


Fig. 12. Vegetation analysis of G-SWIR for 1990 and 2020

From 1990 to 2020, there is a degradation of the environment, especially in the south of the research area and along the spill spots, as demonstrated by the NDVI in Figure 10 which suggests a drop in spectral reflectance, implying that the vegetation has been impacted, making it unhealthy. In Figure 12, the G-SWIR reveals that the vegetation has changed as a result of the oil spill. This is because the NIR spectra are absorbed, and the red band spectra reflected as is characteristic of low chlorophyll plants. Figure SAVI and ARVI2 show a general decline in the spill spots from 1990 to 2020. This is complemented by a growing trend in the same indices away from the spill spots in reaction to the NIR, Green, and Red bands, which indicate low chlorophyll and moisture content, possibly as a result of oil contamination. The rise in G-NIR along the spill points and non-spill points in the study region indicates a greater amount of discrimination between oil-spill-affected and unaffected plants. This suggests a high NIR absorption and a high green band spectral reflection. The considerable discrepancy in these vegetation indices' spatiotemporal analysis, especially in the south of the study area, can be attributed to the fact that the said area has experienced multiple oil spills over the years.

V. CONCLUSION

Oil spill sabotage has been a major issue in the Niger Delta at large and needs to be addressed as quickly as possible due to the environmental implications. The result from the oil spill from the Nigeria Oil Spill Detection and Response Agency (NOSDRA) shows that the total estimated oil spill is 70% while the recovered oil spill is 30%, implying that 40% of the oil spill

is spread across the area of study, causing more harm than good to the environment. Furthermore, the NDVI vegetation indices show a drop in spectral reflectance, implying that the vegetation has been harmed, making it unhealthy. As a result of the oil spill, the vegetation has changed, according to the G-SWIR. This is because the NIR spectra are absorbed, and the red band spectra reflectance is characteristic of low chlorophyll plants. From 1990 to 2020, SAVI and ARVI2 have shown a general decline in the south and near the spill locations, affecting atmospheric conditions. The rise in G-NIR at spill points and non-spill points south of the study area indicates a greater amount of discrimination between oil-spill-affected and non-affected vegetation. This suggests a high NIR absorption and a high green band spectral reflection. The fact that the research area has undergone several oil spills over the years can be attributed to the large variance in the spatiotemporal analysis of these vegetation indices, in the study area.

Recommendation

It is recommended that geospatial techniques be used for oil spill detection and mapping and that the government and IOC protect the environment to reduce the high impact of hydrocarbons on the environment and, most importantly, to sensitize indigenous peoples to the negative effects of this vandalism and the importance of dialogue.

REFERENCES

- [1]. T.A. Abii, P.C. Nwosu, "The Effect of Oil-Spillage on the Soil of Eleme in Rivers State of the Niger-Delta area of Nigeria", Research Journal of Environmental Sciences, vol 3, issue 3, pp. 316-320, 2009.

- [2]. Nelson-Smith, "The effect of oil spills on land and water", in *The Prevention of Oil Pollution*, Dordrecht: Springer, pp 17-34, 1979.
- [3]. UNEP, "Environmental Assessment of Ogoniland." 2011.
- [4]. D.D. Pavanelli, C. Loch, "Mangrove spectra changes induced by oil spills monitored by image differencing of normalised indices: Tools to assist delimitation of impacted areas", *Remote Sens. Appl. Soc. Environ*, vol 12 pp.78–88, 2018.
- [5]. N.N. Onyia, H. Balzter, J.C. Berrio, "Spectral diversity metrics for detecting oil pollution effects on biodiversity in the Niger Delta", *Remote Sensing*, vol 11, issue 22, pp.2662, 2019.
- [6]. J. G. P. W. Clevers, S. M. De Jong, G. F. Epema, F. D. Van Der Meer, W. H. Bakker, A. K. Skidmore, K. H. Scholte, "Derivation of the red edge index using the MERIS standard band setting" *International Journal of Remote Sensing*, vol 23, issue 16, pp 3169-3184, 2002.
- [7]. D. R. Eteh, O.E. Okpobiri, "Floodplain Mapping and Risks Assessment of the Orashi River Using Remote Sensing and GIS in the Niger Delta Region, Nigeria" *Journal of Geographical Research*, Vol 04, issue 02, 2021.
- [8]. Rouse Jr, J. W., Haas, R. H., Schell, J. A., & Deering, D. W "Monitoring the vernal advancement and retrogradation (green wave effect) of natural vegetation" Texas A&M University Remote Sensing Center College Station, Texas, 1973.
- [9]. S.W. Running, C.O. Justice, V. Salomonson, D. Hall, J. Barker, Y.J. Kaufmann, A.H. Strahler, A.R. Huete, J.P. Muller, V. Vanderbilt, Z.M. Wan 1994. "Terrestrial remote sensing science and algorithms planned for EOS/MODIS", *International Journal of Remote Sensing*, vol. 15, issue 17, pp 3587- 3620, 1994.
- [10]. R. Huete, "A soil-adjusted vegetation index (SAVI)." *Remote sensing of environment*, vol 25, issue 3, pp 295-309, 1988.
- [11]. R. Huete, G.Q. Hua, J. Chehbouni, A. V. Leeuwen, "Normalization of multidirectional red and NIR reflectances with the SAVI." *Remote Sensing of Environment*, vol 41, issue 2-3, pp 143- 154, 1992.
- [12]. G. Rondeaux, M. Steven, F. Baret. "Optimization of soil-adjusted vegetation indices." *Remote sensing of environment*, vol 55, issue 2, pp 95-107, 1996.
- [13]. A. Gitelson, Y. J. Kaufman, M. N. Merzlyak, "Use of a green channel in remote sensing of global vegetation from EOS-MODIS", *Remote sensing of Environment*, vol 58. Issue 3, pp 289-298, 1996.
- [14]. Y. J. Kaufman, D. Tanre," Atmospherically resistant vegetation index (ARVI) for EOS-MODIS", *IEEE transactions on Geoscience and Remote Sensing*, vol 30, issue 2, pp 261-270, 1992.
- [15]. R. P. Sripada, R. W. Heiniger, J. G. White, R. Weisz," Aerial color infrared photography for determining late-season nitrogen requirements in corn", *Agronomy Journal*, vol 97 issue 5, pp 1443-1451, 2005.
- [16]. Adamu, K. Tansey, B. Ogutu, "Remote sensing for detection and monitoring of vegetation affected by oil spills", *International Journal of Remote Sensing*, vol 39 issue 11, pp 3628-3645, 2018.
- [17]. Herrmann, A. Karnieli, D. J Bonfil, Y. Cohen, V. Alchanatis, "SWIR-based spectral indices for assessing nitrogen content in potato fields" *International Journal of Remote Sensing*, vol 31, issue 19, pp 5127-5143, 2010.